Supplement of Earth Syst. Sci. Data, 13, 4653–4675, 2021
https://doi.org/10.5194/essd-13-4653-2021-supplement

Supplement of

Global time series and temporal mosaics of glacier surface velocities derived from Sentinel-1 data

Peter Friedl et al.

Correspondence to: Thorsten Seehaus (thorsten.seehaus@fau.de)

Table S1: Tracking and filtering parameters for each region. Window sizes and tracking step sizes are provided in azimuth (az) and range (r) pixels. In some regions, where Sentinel-1A/B 6-day repeat acquisitions are available, the minimum temporal baseline is 12 days for the time prior to 2016 and 6 days for the time after. In cases where the first filtering step of the applied velocity filter by Lüttig et al. (2017) is skipped due to the unavailability of a priori velocity information, the corresponding cell for the factor *w* is left empty.

ID	Region	Window size [r x az]	Tracking step size [r x az]	Minimum temporal baseline [days]	Factor *w* of velocity filter
1	South Georgia	320 x 64	50 x 10	12	-
2	Southern Andes	250 x 50	50 x 10	12	1.5
3	Alaska, Western Canada	250 x 50	50 x 10	12	3
4	Arctic Canada	320 x 64	50 x 10	12/6	1.5
5	Iceland	250 x 50	50 x 10	12/6	1.5
6	European Alps	250 x 50	50 x 10	48	-
7	Svalbard	250 x 50	50 x 10	12/6	3
8	Russian Arctic	512 x 128	50 x 10	12	3
9	Caucasus	250 x 50	50 x 10	48	-
10	High Mountain Asia	250 x 50	50 x 10	12	3
11	New Zealand	250 x 50	50 x 10	48	-
12	Scandinavia	250 x 50	50 x 10	12/6	-

Table S2: Naming convention of scene-pair velocity products and mosaics

Scene-pair velocity products

dis_mag+S1_20200417T061446_0505_1_9_1_9_1_9_S1_20200423T061528_5275_1_9_1_9_1_9+250-50_50-10_0.00-0.08_2_geo_filtered_corrected.tif

a) b) c) d) e)

a) Product type:

dis_mag: velocity magnitude (m d^{-1})
dis_az: azimuth velocity component (m d^{-1})
dis_r: range velocity component (m d^{-1})
dis_ang: displacement angle relative to the sensor's heading angle
dis_N_ang: displacement angle relative to true north
ccp: cross-correlation peak coefficient
ccs: cross correlation function standard deviation
loc_inc: local incidence angle

b) Master scene: S1_yyyymmddThhmmss_Product UID_burst start (sub-swath 1-3)_burst stop (sub-swath 1-3)

c) Slave scene: S1_yyyymmddThhmmss_Product UID_burst start (sub-swath 1-3)_burst stop (sub-swath 1-3)

d) Processing parameters:

window size (r)–window size (az)_step size (r)–step size (az)_initial CCP threshold–final CCP threshold_overs. factor

e) Processing level:

geo: geocoded/orthorectified
geo_filtered: geocoded/orthorectified and filtered
geo_filtered_corrected: geocoded/orthorectified, filtered and corrected

Mosaics

07_mag_stack_2020_04.tif

a) b) c)

a) Region: Region number (see Fig. 1)

b) Product type:

mag_stack: weighted mean of the velocity magnitude (m d^{-1})
mag_sd_stack: weighted standard deviation of the velocity magnitude (m d^{-1})
mag_se_stack: weighted standard error of the velocity magnitude (m d^{-1})
y_stack: weighted mean of the y velocity component (m d^{-1})
y_sd_stack: weighted standard deviation of the y velocity component (m d^{-1})
y_se_stack: weighted standard error of the y velocity component (m d^{-1})
x_stack: weighted mean of the x velocity component (m d^{-1})
x_sd_stack: weighted standard deviation of the x velocity component (m d^{-1})
x_se_stack: weighted standard error of the y velocity component (m d^{-1})
N_ang_stack: mean displacement angle relative to true north
count_stack: number of measurements per pixel
date_stack: mean acquisition date per pixel (days since 1 January 1900)
time_sep_stack: mean time separation per pixel (days)

c) Date: yyyy (annual mosaic), yyyy_mm (monthly mosaic)

Section S1: Comparison between Sentinel-1 and TerraSAR-X velocity fields at a narrow mountain glacier.

We carried out a comparison of Sentinel-1 velocity measurements with a velocity field derived from high resolution TerraSAR-X data at the glacier tongue of Yazghil Glacier in December 2015. Yazghil Glacier is a rather narrow (~800 m) but partly fast flowing (up to 2.5 m d^{-1}) mountain glacier in the Karakorum, allowing an analysis of the impact of the spatial resolution and the tracking window size on the velocity estimates.

We applied the same routine to the TerraSAR-X data as for the comparison on Svalbard (Section 2.5). The resulting velocity fields from both sensors are illustrated in Figure S1. We selected 4 profiles (one along and three cross glacier profiles) to further investigate the difference between the resulting products (Figure S2). As seen in Figure S1, the Sentinel-1 product has a lower spatial coverage on glacier. Moreover, the velocities in the lateral zones of the glaciers are often lower for Sentinel-1 as for TerraSAR-X. These findings are supported by the velocity measurements along the glacier profiles (Figure S2). In particular the plot of profile 1 indicates that there is a general trend for Sentinel-1 products to underestimate the flow velocity, in particular at the slow-moving section towards the terminus and for the small-scale high velocity section.

The larger tracking window size for Sentinel-1 (250 x 50 pixels at about 4x20 m ground resolution, see Table S1 vs. 128x128 pixels at about 3x3 m ground resolution for TerraSAR-X), explains these limitations. For Sentinel-1, more stable areas around the glacier are covered by the tracking window, affecting the offset estimation and leading to the revealed but also expected underestimation of the glacier velocities towards the margins. In a similar way, the relatively small zone with high glacier velocities (>1 m d^{-1} according to the TerraSAR-X data) are partly averaged out by the lower resolution and larger tracking window size of the Sentinel-1 data.

The tracking window sizes were carefully selected to obtain good results for the majority of the glaciers in the respective region. However, for such a global database, there are always certain limitations and not all details can be fully resolved. Considering the results from this comparison and experience from visible inspection of further Sentinel-1 products, we conclude that it is very likely, that the flow velocities at glaciers narrower 1 km are underestimated, in particular towards the margins, and that high velocity variations at scales of 1-2 km and below may be partly averaged out.

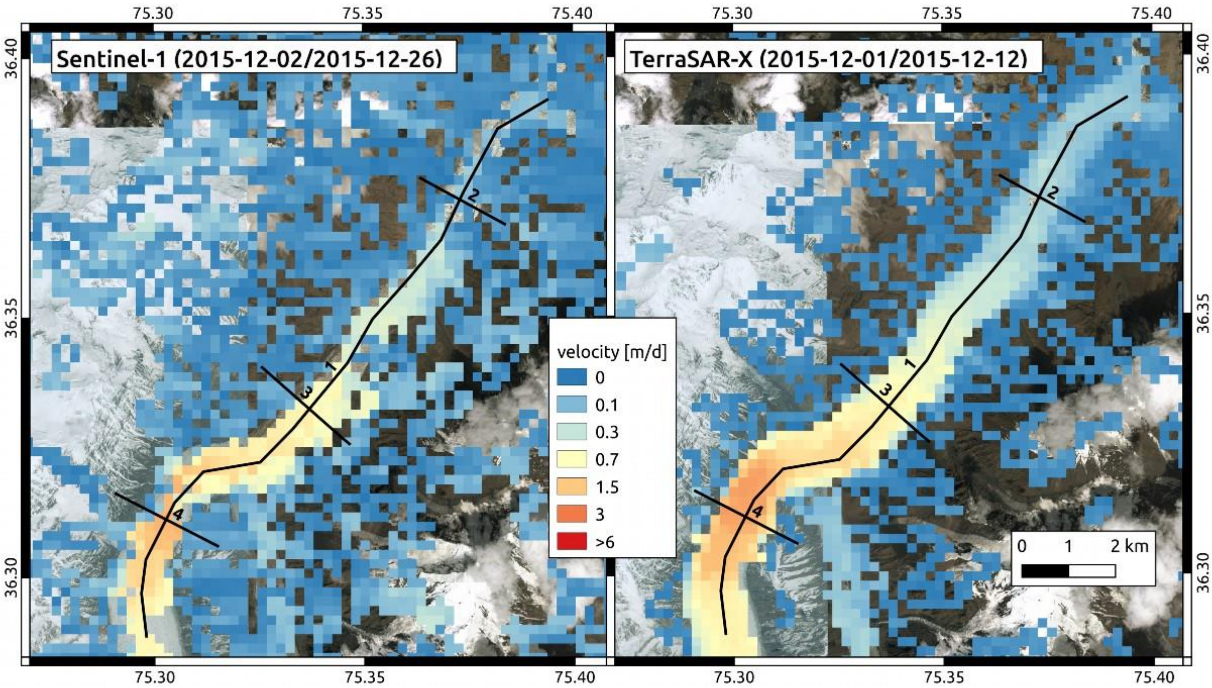

Figure S1: Surface velocity fields at Yazghil Glacier, Karakorum, derived from Sentinel-1 (left panel) and TerraSAR-X (right panel) imagery in December 2015. Black lines indicate profiles for velocity measurements, see Figure S2. Background: Bing Satellite

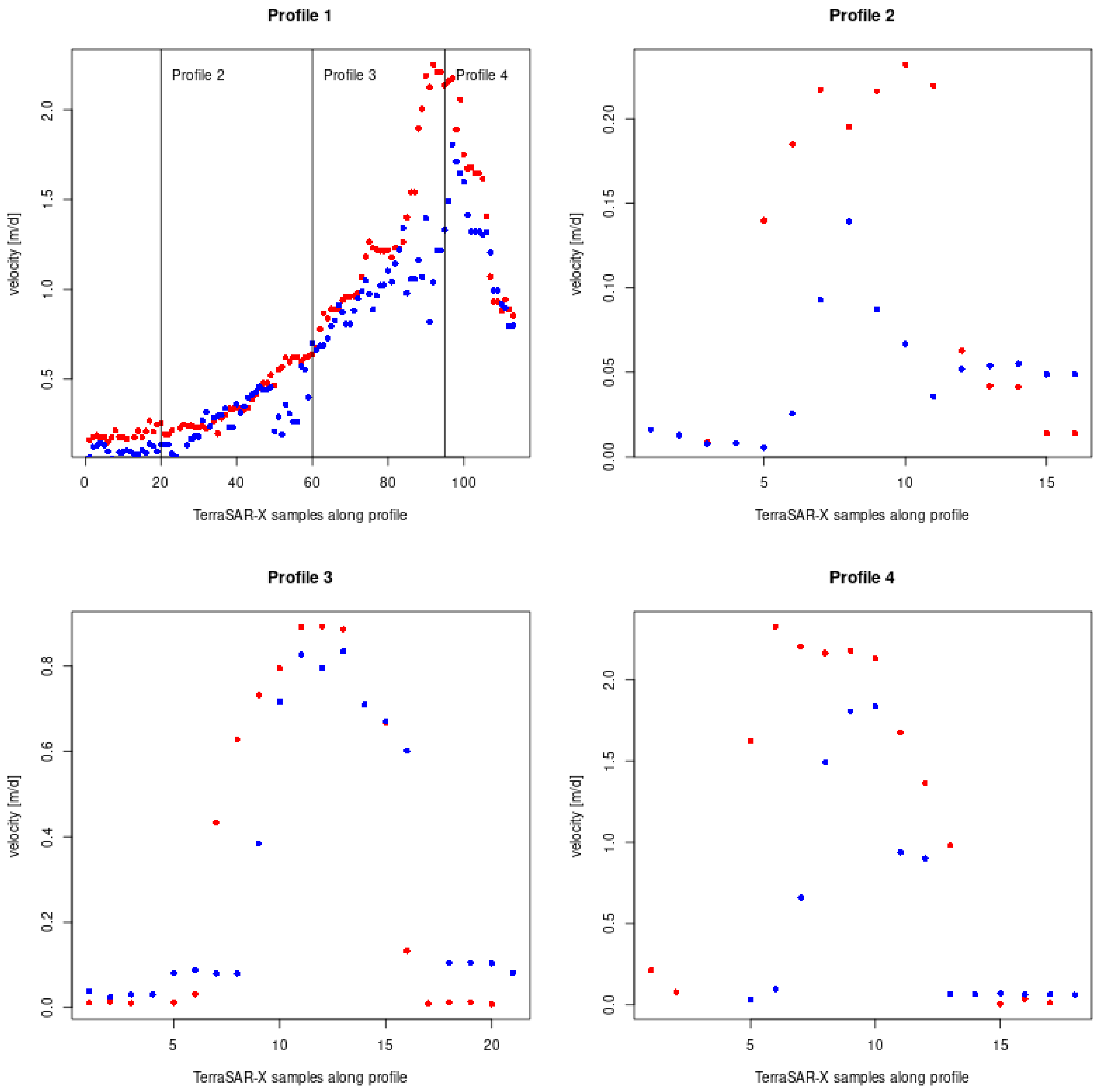

Figure S2: Velocity estimates based on Sentinel-1 (blue dots) and TerraSAR-X (red dots) along profiles on Yazghil Glacier (See Figure S1) in December 2015. Vertical lines in the top right panel indicate crossing points with other profiles.

References

Lüttig, C., Neckel, N., and Humbert, A.: A Combined Approach for Filtering Ice Surface Velocity Fields Derived from Remote Sensing Methods, Remote Sensing, 9, 1062, https://doi.org/10.3390/rs9101062, 2017.